

A Dual-Slot Microwave Antenna for More Spherical Ablation Zones: Ex Vivo and in Vivo Validation¹

Jason Chiang, MS
Kieran A. Hynes
Mariajose Bedoya, BS
Christopher L. Brace, PhD

Purpose:

To compare the performance of a microwave antenna design with two annular slots to that of a monopole antenna design in creating a more spherical ablation zone.

Materials and Methods:

Animal care and use committee approval was obtained before in vivo experiments were performed. Microwave ablation zones were created by using dual-slot and monopole control antennas for 2, 5, and 10 minutes at 50 and 100 W in ex vivo bovine livers. Dual-slot and monopole antennas were then used to create ablation zones at 100 W for 5 minutes in in vivo porcine livers, which also underwent intraprocedural imaging. Ablation diameter, length, and aspect ratio (diameter ÷ length) were measured at gross pathologic examination and compared at each combination of power and time by using the paired Student *t* test. A *P* value less than .05 was considered to indicate a significant difference. Aspect ratios closer to 1 reflected a more spherical ablation zone.

Results:

The dual-slot antenna created ablation zones with a higher aspect ratio at 50 W for 2 minutes (0.75 vs 0.53, *P* = .003) and 5 minutes (0.82 vs 0.63, *P* = .053) than did the monopole antenna in ex vivo liver tissue, although the difference was only significant at 2 minutes. At 100 W, the dual-slot antenna had a significantly higher aspect ratio at 2 minutes (0.52 vs 0.42, *P* = .002). In vivo studies showed significantly higher aspect ratios at 100 W for 5 minutes (0.63 vs 0.53, respectively, *P* = .029). Intraprocedural imaging confirmed this characterization, showing higher rates of ablation zone growth and heating primarily at the early stages of the ablation procedure when the dual-slot antenna was used.

Conclusion:

The dual-slot microwave antenna created a more spherical ablation zone than did the monopole antenna both in vivo and ex vivo liver tissue. Greater control over power delivery can potentially extend the advantages of the dual-slot antenna design to higher power and longer treatment times.

© RSNA, 2013

¹From the Departments of Radiology (J.C., C.L.B.), Biomedical Engineering (J.C., M.B., C.L.B.), and Chemistry (K.A.H.), University of Wisconsin, 1111 Highland Ave, WIMR 1303-0, Madison, WI 53705. From the 2012 RSNA Annual Meeting. Received September 21, 2012; revision requested November 19; revision received January 5, 2013; accepted January 21, 2013; final version accepted January 23. Address correspondence to C.L.B. (e-mail: clbrace@wisc.edu).

© RSNA, 2013

Percutaneous tumor ablation is a minimally invasive procedure that destroys cancerous tissue in situ with cytotoxic thermal energy. Thermal ablation procedures are associated with quicker recovery and fewer complications compared with surgical resection, and these are now critical procedures in the management of early-stage hepatocellular carcinoma, hepatic metastases, renal cell carcinoma, peripheral lung nodules, osteoid osteomas, and osteosarcomas (1,2). Although radiofrequency ablation is the most widely used ablation modality, its use is limited by difficulties in heating charred or desiccated tissue and its poor performance near blood vessels. Such limitations to heating can lead to potentially inadequate ablation zones and a higher rate of local tumor progression than those with resection (2,3). Microwave ablation, on the other hand, has been shown to heat larger volumes of tissue to greater temperatures, potentially increasing procedural efficacy (4–6).

Interstitial antennas deliver power from the microwave generator to the target tissue. The pattern of heating around the antenna varies with antenna design, but high-power delivery can also promote electric field propagation along the proximal shaft during an ablation treatment (7–11). This effect can cause procedural complications such as body-wall burns and can restrict where the applicator can be placed (12–14). Such complications may be reduced by

Advances in Knowledge

- The dual-slot microwave antenna can create a more spherical ablation zone than the monopole antenna can in ex vivo and in vivo liver tissue.
- Substantial water vapor is formed and can be visualized with intraprocedural CT imaging to characterize ablation zone growth during microwave heating.
- Differences in heating patterns produced by different antenna designs may be minimized by using high powers or long treatment times.

cooling the skin surface and limiting the power or duration of the treatment; however, these techniques add procedural complexity and reduce the size of the ablation zone (15). Antenna cooling can effectively reduce shaft heating but has minimal effect against ablation zone elongation (16–19).

A dual-slot antenna comprising two coaxial, annular slots at the distal tip was recently shown to inhibit proximal electric field propagation and, therefore, to shorten the length of ex vivo ablations (20). However, the antenna in that study was created from relatively malleable coaxial cables without active shaft cooling, making it unsuitable for clinical use. A dual-slot antenna was recently developed that incorporates a rigid, sharpened tip and internal water cooling to facilitate percutaneous use while maintaining its original performance. The goal of this study was to compare the performance of a microwave antenna design with two annular slots to that of a monopole antenna design in creating a more spherical ablation zone.

Materials and Methods

The microwave antenna devices used in this study incorporate aspects of multiple patents pending. No industrial support was provided for this study. Author C.L.B. is a founder, shareholder, and consultant for NeuWave Medical. Study data and publication information were controlled by J.C.

By using a parametric analysis similar to that used in previous work, we designed a dual-slot antenna with a built-in shaft, cooling channels, and a coaxial feed separate from the trocar tip to simplify fabrication. The optimal cooled design provided a heating pattern and power delivery efficiency similar to those of the uncooled design previously described (20). A cooled monopole antenna served as a control

Implication for Patient Care

- A more spherical, less elongated ablation zone can potentially lead to increased ablation precision and reduced complications.

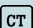

antenna for comparison of ablation performance (Fig 1). Both antennas were fabricated by using a thin coaxial antenna (UT-020C; Micro-Coax, Pottstown, Pa), an alumina ceramic tip to enhance rigidity (McDanel Advanced Ceramic Technology, Beaver Falls, Pa), and a 17-gauge steel catheter to create the cooling channel (MicroGroup, Medway, Mass). Antennas were fabricated by two authors (K.A.H. and J.C., each with 2 years of experience).

Microwave power was delivered by means of a continuous-wave 2.45-GHz magnetron source (MG300; CouberMuegge, Norwalk, Conn) and transferred to the antenna via a 6-foot RG-400 coaxial cable. Cable losses were measured by using a wideband power sensor (Birds Electronic, Solon, Ohio) and were used to recalibrate the generator output to ensure delivery of the prescribed power into the tissue.

Ex Vivo Bovine Liver Ablation

Microwave antenna performance was initially validated by using ex vivo bovine liver tissue. The liver was sectioned into blocks measuring $6 \times 6 \times 9$ cm and was warmed to room temperature before each experiment. The microwave generator was set to deliver 50 W and 100 W for 2, 5, and 10 minutes for each antenna. Six samples were performed (K.A.H. and M.B., both with 2 years of experience) per power and time

Published online before print

10.1148/radiol.13122128 Content codes:  

Radiology 2013; 268:382–389

Author contributions:

Guarantors of integrity of entire study, J.C., C.L.B.; study concepts/study design or data acquisition or data analysis/interpretation, all authors; manuscript drafting or manuscript revision for important intellectual content, all authors; approval of final version of submitted manuscript, all authors; literature research, J.C., K.A.H., C.L.B.; clinical studies, J.C., K.A.H., C.L.B.; experimental studies, all authors; statistical analysis, J.C., C.L.B.; and manuscript editing, J.C., K.A.H., C.L.B.

Funding:

This research was supported by the National Institutes of Health (grants 1 R01 CA142737 and UL1TR000427).

Conflicts of interest are listed at the end of this article.

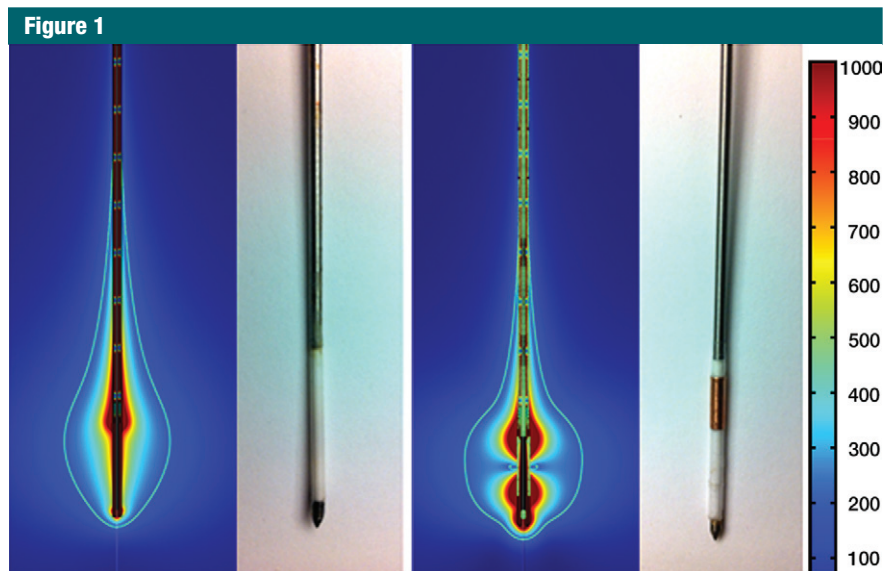


Figure 1: Numeric modeling image and photograph of monopole antenna (left) and dual-slot antenna (right). In modeling images, color bar represents electric field intensity from 100 to 1000 V/m. Monopole antenna shows electric field emanating from tip of steel catheter; dual-slot antenna shows electric field from each of its slots. White line represents volumetric heating rate of $3 \times 10^4 \text{ W/m}^3$, giving a visual approximation of what ablation zone may look like in liver tissue. Note decreased active heating on shaft of dual-slot antenna compared with that of monopole.

combination for a total of 36 dual-slot and 36 monopole ablations. The ablation zone was sliced along the antenna axis for gross pathologic analysis. The slices were scanned optically and images were stored for analysis by using ImageJ 1.43u software (US National Institutes of Health, Bethesda, Md). The maximum dimension of the ablation zone transverse to the antenna was defined as the ablation diameter, and the maximum dimension along the antenna insertion path was considered the ablation length. The aspect ratio was defined as the diameter divided by the length. An aspect ratio approaching 1 indicates that the ablation length is approaching that of its diameter, indicating a more spherical ablation zone.

In Vivo Porcine Liver Ablation

All studies were conducted with approval from our institutional animal care and use committee and were compliant with National Research Council guidelines (21). A total of four ablations (two with the dual-slot and two with monopole antennas) were created (J.C.

and a veterinary technician, with 2 and 12 years of experience, respectively) by using 100 W for 5 minutes in each of six female domestic swine with a weight range of 80–90 kg (Arlington Farms, Arlington, Wis) for a total of 24 ablations (12 monopole and 12 dual-slot). For each animal, half ($n = 2$) of the ablations for each experimental arm were performed in the medial lobes and the other half were performed in the lateral lobes to account for differences in perfusion rates. Ablations that protruded beyond the parenchyma of the tissue or in which antenna failure occurred were excluded from the results. After exclusion of incomplete ablation zones, there were eight dual-slot ablations and eight monopole ablation zones in the *in vivo* study.

Animals were sedated with intramuscular tiletamine hydrochloride and zolazepam hydrochloride (7 mg/kg, Telazol, Fort Dodge, Iowa) and xylazine hydrochloride (2.2 mg/kg, Xyla-Ject; Phoenix Pharmaceutical, St Joseph, Mo). Anesthesia was maintained with inhaled 1%–2% isoflurane

(Halocarbon Laboratories, River Edge, NJ). An ear vein was cannulated with a 20-gauge angiographic catheter for administration of intravenous fluids.

After ablation, animals were sacrificed by means of an intravenous injection of pentobarbital sodium and phenytoin sodium (0.2 mL/kg, Beuthanasia-D; Schering-Plough, Kenilworth, NJ). The liver was removed and sectioned along the axis of each antenna. Image analysis was performed in the same way as with *ex vivo* tissue.

Unenhanced computed tomographic (CT) imaging was used to assess ablation growth in two of the animals. Before the ablation, a roadmap CT scan was obtained of the entire liver. During the ablation, CT data were acquired every 30 seconds. (120 kV, 200 mA, 512×512 , 1:1 helical pitch, 5 mm section thickness). A threshold was set at 35 HU, which was approximately 16 HU below the background liver attenuation with postprocessing software (Volume Viewer version 3.1; Advantage Windows version 4.5, GE Medical Systems, Wis) to detect and monitor ablation zone area growth at each time point. This value was chosen on the basis of previous CT studies, which showed the average 16-HU difference between an ablated lesion from radiofrequency ablation and the background tissue (22). The final threshold image was compared with gross pathologic results to confirm the validity of using our threshold technique to monitor ablation growth. The central hypoattenuating region, which was heated and gaseous surrounding the emission point, was also monitored, and diameter, length, and overall area were recorded at each time point.

Statistical Analysis

To ensure that there were no probe-lobe interaction effects, we compared the ablation zone characteristics produced by each antenna while accounting for placement in the lobe. Because the effects seemed additive, we averaged the ablation zone dimensions over lobes by probe type to produce a single monopole and dual-slot pair per animal. Differences in mean diameter, length, and aspect ratio between the dual-slot and monopole

Figure 2

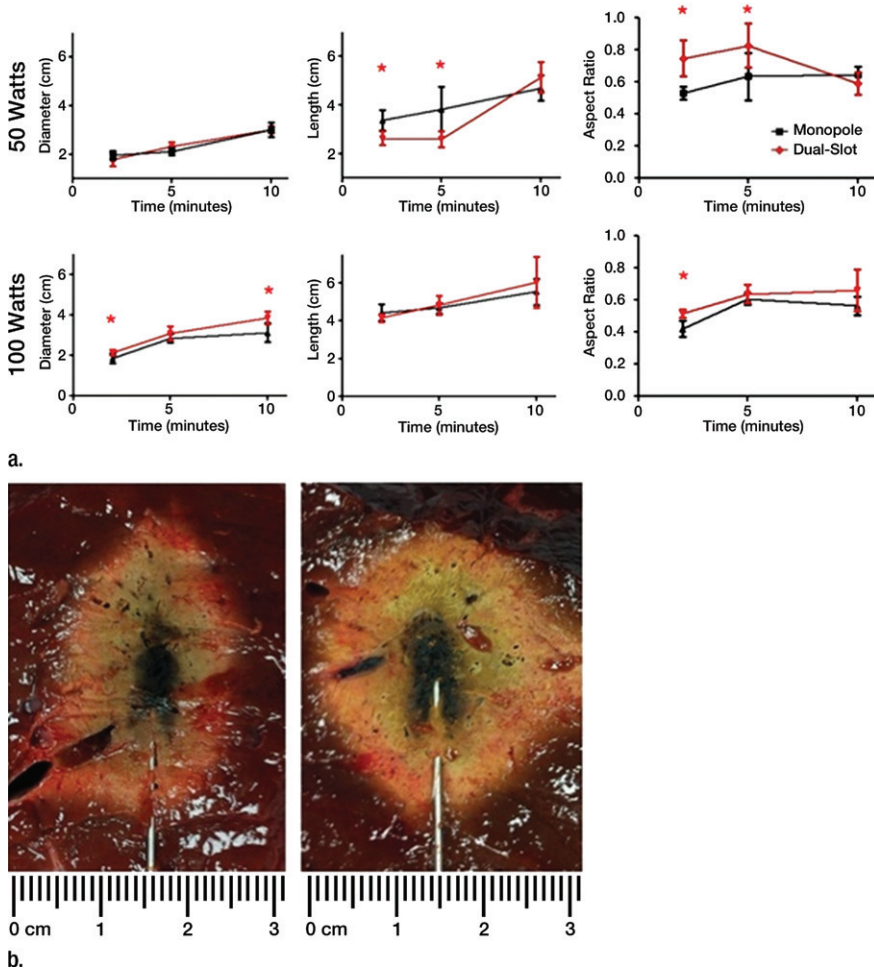


Figure 2: (a) Graphs show ablation diameter, length, and aspect ratio of ex vivo ablations comparing dual-slot with monopole antennas. Solid dots represent sample mean, and horizontal line segments represent standard deviation. * = significant difference ($P < .05$). (b) Sample ablation zone created by dual-slot (left) and monopole (right) antennas at 100 W for 5 minutes. Dual-slot antenna created significantly shorter and more spherical ablation zone than did monopole antenna at 50 W for 2 and 5 minutes. Dual-slot antenna created a significantly wider and more spherical ablation zone compared with monopole antenna at 100 W for 2 minutes.

antenna designs were identified among the power and treatment length combinations by using a paired Student *t* test. The paired Student *t* test was considered appropriate after validating approximately equal variances and symmetric distribution among comparison groups. *P* values less than .05 were considered to indicate a significant difference. Statistical analysis was performed by using Graphpad Prism version 5.04 (La Jolla, Calif) with assistance from the departmental statistician.

Results

Ex Vivo Results

Power and time dose responses of the monopole and dual-slot antennas are shown in Figure 2. At 50 W, the dual-slot antenna created ablation zone diameters similar to those of the monopole at 2 minutes ($1.95 \text{ cm} \pm 0.18$ vs $1.79 \text{ cm} \pm 0.27$, respectively; $P = .278$), 5 minutes ($2.12 \text{ cm} \pm 0.14$ vs $2.32 \text{ cm} \pm 0.18$; $P = .078$), and 10 minutes ($3.01 \text{ cm} \pm 0.29$ vs $3.02 \text{ cm} \pm$

0.16 ; $P = .987$). With respect to ablation length, the dual-slot antenna created significantly shorter ablation zones compared with those of the monopole antenna at 2 minutes ($2.64 \text{ cm} \pm 0.30$ vs $3.38 \text{ cm} \pm 0.42$; $P = .007$) and 5 minutes ($2.61 \text{ cm} \pm 0.34$ vs $3.83 \text{ cm} \pm 0.92$; $P = .020$), but not at 10 minutes ($5.14 \text{ cm} \pm 0.64$ vs $4.71 \text{ cm} \pm 0.51$, respectively; $P = .225$). Accordingly, the combination of equivalent diameters and shorter ablation lengths led to a greater aspect ratio for dual-slot ablation zones at 2 minutes (0.75 ± 0.11 vs 0.53 ± 0.04 , $P = .003$) and 5 minutes (0.82 ± 0.13 vs 0.63 ± 0.14 , $P = .053$), but not at 10 minutes (0.59 ± 0.07 vs 0.64 ± 0.05 , $P = .168$).

At 100 W, the dual-slot antenna created ablation zones with diameters greater than those created by the monopole antenna at all of the time points ($2.14 \text{ cm} \pm 0.15$ vs $1.86 \text{ cm} \pm 0.24$ at 2 minutes, $P = .032$; $3.07 \text{ cm} \pm 0.35$ vs $2.80 \text{ cm} \pm 0.19$ at 5 minutes, $P = .077$; $3.86 \text{ cm} \pm 0.32$ vs $3.12 \text{ cm} \pm 0.48$ at 10 minutes, $P = .017$), but the difference was only significant at 2 and 10 minutes. On the other hand, no differences were noted in ablation lengths between the dual-slot and monopole antennas at any of the time points ($4.16 \text{ cm} \pm 0.20$ vs $4.44 \text{ cm} \pm 0.44$ at 2 minutes, $P = .186$; $4.83 \text{ cm} \pm 0.50$ vs $4.62 \text{ cm} \pm 0.31$ at 5 minutes, $P = .354$; $6.04 \text{ cm} \pm 1.35$ vs $5.55 \text{ cm} \pm 0.69$ at 10 minutes, $P = .458$). Collectively, the greater ablation diameter of the dual-slot antenna with the equivalent ablation lengths led to a significantly higher aspect ratio than that of the monopole antenna at only 2 minutes (0.52 ± 0.03 vs 0.42 ± 0.05 , $P = .002$), with the aspect ratios being statistically similar at 5 minutes (0.64 ± 0.05 vs 0.61 ± 0.03 , $P = .191$) and 10 minutes (0.66 ± 0.13 vs 0.56 ± 0.06 , $P = .136$).

In Vivo Results

In vivo studies confirmed the trends shown in the ex vivo studies (Fig 3a). The dual-slot antenna created a significantly greater diameter ($2.85 \text{ cm} \pm 0.45$ vs $2.35 \text{ cm} \pm 0.42$, respectively; $P = .034$) and a slightly shorter length ($4.47 \text{ cm} \pm 0.71$ vs $4.59 \text{ cm} \pm 0.81$,

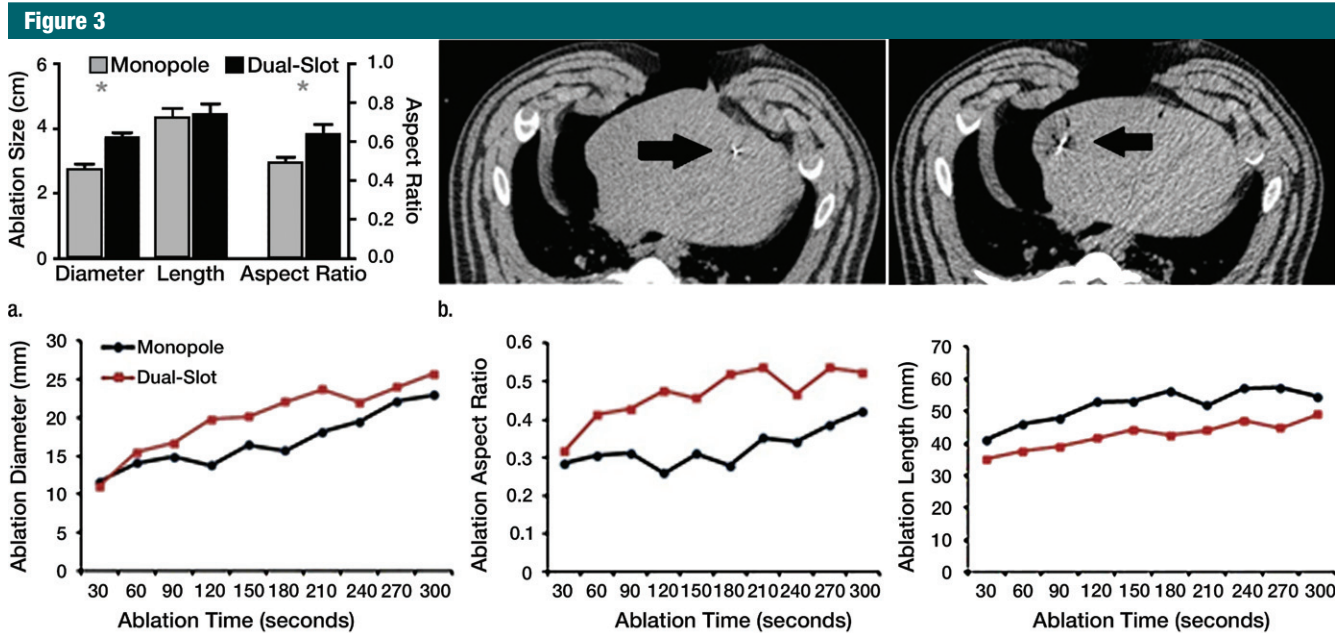


Figure 3: (a) Bar graph shows in vivo diameter, length, and aspect ratio of dual-slot and monopole antennas at 100 W for 5 minutes. Dual-slot antenna created ablation zones that were significantly wider and more spherical than those created by using monopole antennas. This is consistent with trends found in power and treatment length in ex vivo tissue. * = significant difference ($P < .05$). (b) Sample intraprocedural images show microwave antenna placement in porcine liver. (c) Intraprocedural monitoring of ablation zone diameter, length, and aspect ratio during in vivo ablation with dual-slot and monopole antennas.

respectively; $P = .597$), leading to a significantly greater aspect ratio compared with the monopole antenna (0.63 ± 0.08 vs 0.53 ± 0.08 , respectively; $P = .029$).

Intraprocedural CT with thresholding confirmed these trends, with the final ablation zone of the dual-slot antenna showing a greater diameter and shorter ablation zone than those of the monopole antenna. Intraprocedural CT also showed differences in the ablation zone growth pattern. The diameter of the dual-slot ablation zone was similar to that of the monopole at the start of the procedure but grew much faster than that of the monopole until 4 minutes into the procedure. After this point, the growth rate of the diameter slowed down, while the monopole ablation diameter continued to grow in a linear fashion. The ablation length of the dual-slot antenna was shorter than that of the monopole antenna at nearly every time point, although the growth rate was approximately the same. The combination of the dual-slot antenna creating a wider ablation zone and

maintaining a shorter ablation length led to the dual-slot antenna having a greater aspect ratio at every time point during the 5-minute ablation (Fig 3c).

Intraprocedural CT also demonstrated differences in heating pattern, which was demarcated by a coarse outline of a hypoattenuating region (less than -300 HU), most likely representing water vaporization at the interface between tissue and the antenna heating element (Fig 4a). The hypoattenuating region was noted initially near the base of the monopole radiating segment, approximately 20 mm proximal to the antenna tip. The dual-slot antenna created a similar region approximately 5 mm proximal to the tip. That region grew slightly along the proximal antenna shaft but to a lesser degree than that of the monopole. The growth rate of the hypoattenuating area varied between the antenna designs (Fig 4b). The dual-slot antenna created a larger hypoattenuating region at all of the time points than did the monopole, suggesting a higher rate of local heating and subsequent

vaporization. In terms of growth rate, both antennas created most of the hypoattenuating region in the first 2 minutes; the dual-slot antenna appeared to plateau within 3 minutes, but the monopole antenna's hypoattenuating region continued to grow steadily until 5 minutes.

Discussion

In our study, we characterized the ablation zone produced by a water-cooled dual-slot antenna in a preclinical liver tissue model. Compared with a cooled monopole antenna, dual-slot ablations had greater diameter-to-length aspect ratios, particularly for treatment times less than 5 minutes. Greater aspect ratios were attributed to shorter ablation lengths at lower power and increased ablation diameters at higher power. Similar trends were observed in vivo, although ablation zones were markedly smaller and more spherical than those made in ex vivo tissue due to the presence of perfusion.

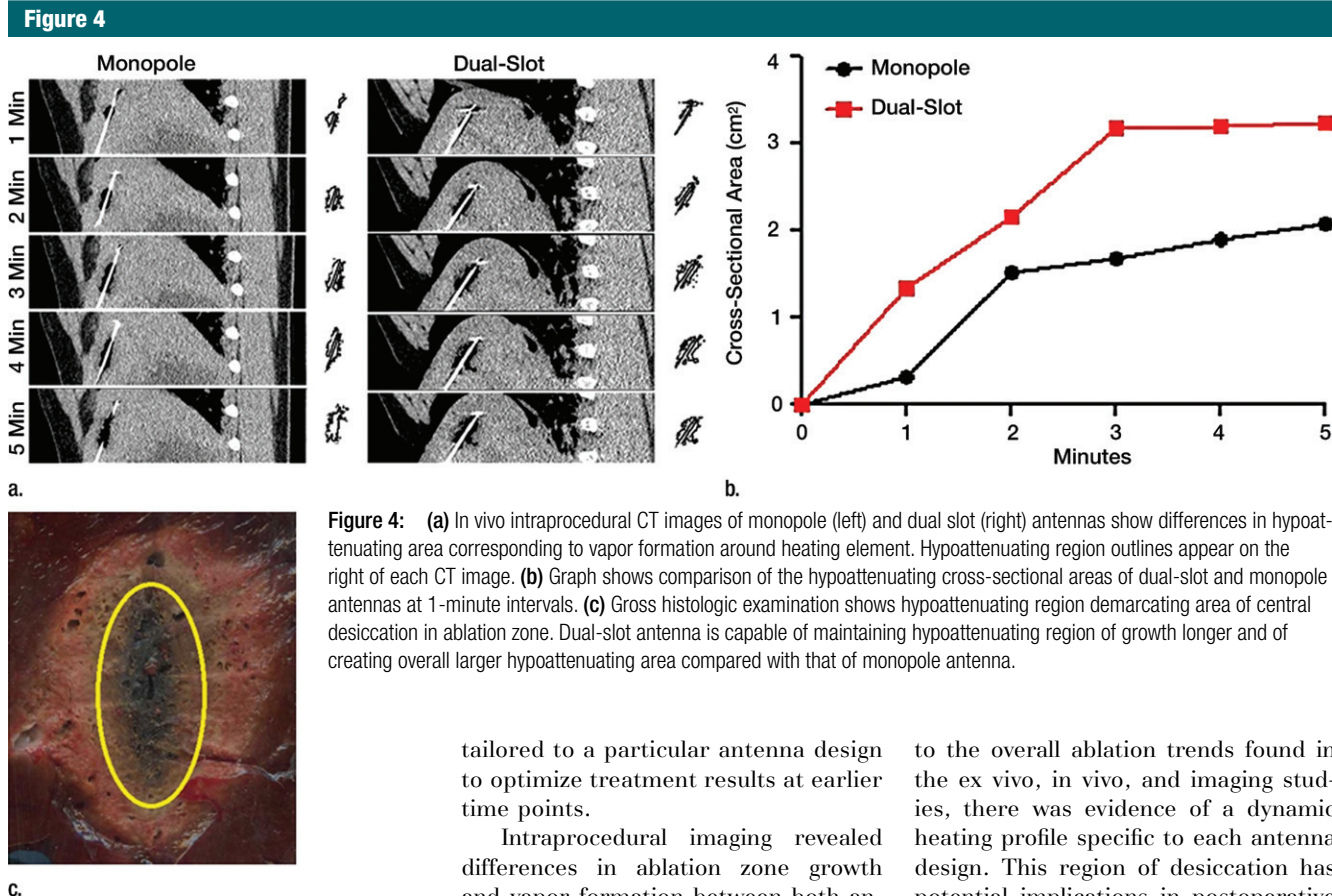


Figure 4: (a) In vivo intraprocedural CT images of monopole (left) and dual slot (right) antennas show differences in hypoattenuating area corresponding to vapor formation around heating element. Hypoattenuating region outlines appear on the right of each CT image. (b) Graph shows comparison of the hypoattenuating cross-sectional areas of dual-slot and monopole antennas at 1-minute intervals. (c) Gross histologic examination shows hypoattenuating region demarcating area of central desiccation in ablation zone. Dual-slot antenna is capable of maintaining hypoattenuating region of growth longer and of creating overall larger hypoattenuating area compared with that of monopole antenna.

Our results suggest that antenna design may be more effective at actively controlling the ablation shape for the first few minutes of the ablation. After then, effects such as thermal conduction and tissue property changes may eliminate earlier differences. Schramm et al (23) predicted only a small influence of thermal conduction on microwave ablations, but that study did not account for water vaporization or associated heat transfer. Ji et al (24) noted an increase in the ablation zone length over time when accounting for dielectric property changes caused by vaporization and desiccation around the antenna shaft. Our study results appear to have confirmed those findings, as was shown in the lack of difference between dual-slot and monopole ablation aspect ratios at 10 minutes. This evidence suggests that power delivery techniques may need to be

tailored to a particular antenna design to optimize treatment results at earlier time points.

Intraprocedural imaging revealed differences in ablation zone growth and vapor formation between both antennas, which may contribute to the final gross pathologic results. The dual-slot ablation length started out shorter than that of the monopole and maintained that difference throughout the procedure, with both ablation zones growing at approximately the same rate. Although our gross pathologic studies revealed only part of the entire ablation growth curve, these imaging results confirmed the ablation trends found in both the in vivo and ex vivo studies.

Zones of extreme hypoattenuation that corresponded to water vaporization in the tissue were also monitored near the ablation applicator (24). The vapor zones corresponded approximately to the centrally blackened, desiccated area in the middle of the ablation zone, which appeared to reach much higher temperatures compared with the transition zone, which was darker but maintained its structure on gross pathologic examination. Similar

to the overall ablation trends found in the ex vivo, in vivo, and imaging studies, there was evidence of a dynamic heating profile specific to each antenna design. This region of desiccation has potential implications in postoperative pathology or monitoring in demarcating areas where cells potentially experience thermal fixation (25).

The ablation zones found with the dual-slot antenna were comparable to those found with other cooled antenna designs. Ablation zones with the monopole and dual-slot antennas were both larger than those of the cooled dipole antennas as reported by Sun et al (16) and Zhou et al (26) in both diameter and length at 50 W, but comparable dimensions were reported at the higher powers (80–100 W for 10 minutes). These studies confirm that antenna designs create distinct ablation zones at lower powers but become similar to each other at higher powers. Hines-Peralta et al (19) characterized a cooled large-gauge antenna that created much wider and longer ablation zones compared with the ones reported here, but they used an antenna that was much greater in diameter. Cavagnaro et al (18) reported a validation

study with a cooled, choked dipole design, which added a third outer conductor over an entire dipole antenna. Their *ex vivo* results showed an increasingly spherical ablation zone as ablation length continued up until 15 minutes at lower powers (20–60 W). At shorter time periods, the choked-dipole antenna design created ablation zones that were more elongated, with comparable diameters compared with those created by the dual-slot antenna. Comparisons between *ex vivo* and *in vivo* studies were consistent with these previous studies, where the *in vivo* ablation zones were noticeably smaller than those created in *ex vivo* tissue. One exception was with the Hines-Peralta study (27), where the *in vivo* ablation zones were larger than the *ex vivo* ablation zones for all 150-W ablations less than 10 minutes long. These variations could potentially have been attributed to the condition of the liver or more rapid tissue contraction, which were not evaluated.

There were certain limitations to our study. First, the cooled monopole and dual-slot antennas were fabricated by hand, limiting tolerances to approximately 1 mm and producing some variation between antennas. However, such variations were not likely to influence the treatment more than variations between tissue properties, perfusion rates, and placement locations. Second, the *ex vivo* and *in vivo* tissue often had vasculature that disrupted the shape of the ablation zone. Microwave energy is capable of overcoming large vascular heat sinks and expanding the ablation zone through extreme vessel heating, adding variability to our ablation geometry measurements (28). Third, our *in vivo* studies were limited in that they were not performed in a tumor-specific model, which would have a different vasculature appearance, as well as different thermal and electric properties. However, tumor models for large animals are not widely available or feasible for such characterization studies. Last, our *in vivo* data were limited to a single power setting. Preliminary testing at 50 W created ablation zones that were highly susceptible

to the effect of perfusion and not useful for antenna characterization. The use of higher powers could add further detail and increase the performance of the two antennas.

In conclusion, the cooled dual-slot antenna created more spherical ablation zones than did a cooled monopole antenna in both *ex vivo* and *in vivo* liver models. The ablation zones of both antennas became more elongated at higher powers and longer treatment times. Intraprocedural CT studies that use a threshold function to observe the ablation zone growth were not consistent with the gross pathologic results. Further refinement with this method of observing ablation growth at unenhanced CT is required to obtain more consistent monitoring. Intraprocedural studies revealed a distinct hypoattenuating region of vapor that was unique to each antenna design, demonstrating different rates of volumetric ablation growth between the monopole and dual-slot antennas. This vaporization pattern potentially can be used to characterize microwave antenna performance. Differences between antenna designs may gradually diminish with increasing power or treatment duration. Adjusting the power delivery algorithm may more fully exploit the theoretical advantages of specific antenna designs.

Acknowledgments: The authors thank Lisa Sampson, BS, for her assistance in experimental setup and Alejandro Muñoz del Rio, PhD, for his assistance with statistics.

Disclosures of Conflicts of Interest: J.C. Financial activities related to the present article: none to disclose. Financial activities not related to the present article: patents pending with support of the Wisconsin Alumni Research Foundation. Other relationships: none to disclose. K.A.H. No relevant conflicts of interest to disclose. M.B. No relevant conflicts of interest to disclose. C.L.B. Financial activities related to the present article: none to disclose. Financial activities not related to the present article: payment for consultancy from NeuWave Medical, Triagenics, and Edwin Hlavka, stock options from NeuWave Medical. Other relationships: none to disclose.

References

1. Wong R, Frenette C. Updates in the management of hepatocellular carcinoma. *Gastroenterol Hepatol (N Y)* 2011;7(1):16–24.

2. Abu-Hilal M, Primrose JN, Casaril A, McPhail MJ, Pearce NW, Nicoli N. Surgical resection versus radiofrequency ablation in the treatment of small unifocal hepatocellular carcinoma. *J Gastrointest Surg* 2008;12(9):1521–1526.
3. Ayav A, Germain A, Marchal F, et al. Radiofrequency ablation of unresectable liver tumors: factors associated with incomplete ablation or local recurrence. *Am J Surg* 2010;200(4):435–439.
4. Andreano A, Huang Y, Meloni MF, Lee FT Jr, Brace C. Microwaves create larger ablations than radiofrequency when controlled for power in *ex vivo* tissue. *Med Phys* 2010;37(6):2967–2973.
5. Brace CL. Microwave tissue ablation: biophysics, technology, and applications. *Crit Rev Biomed Eng* 2010;38(1):65–78.
6. Brace CL. Radiofrequency and microwave ablation of the liver, lung, kidney, and bone: what are the differences? *Curr Probl Diagn Radiol* 2009;38(3):135–143.
7. Labonte S, Blais A, Legault SR, Ali HO, Roy L. Monopole antennas for microwave catheter ablation. *IEEE Trans Microw Theory Tech* 1996;44(10):1832–1840.
8. Hurter W, Reinbold F, Lorenz WJ. A dipole antenna for interstitial microwave hyperthermia. *IEEE Trans Microw Theory Tech* 1991;39(6):1048–1054.
9. Brace CL, Laeseke PF, van der Weide DW, Lee FT. Microwave ablation with a triaxial antenna: results in *ex vivo* bovine liver. *IEEE Trans Microw Theory Tech* 2005;53(1):215–220.
10. Bertram JM, Yang D, Converse MC, Webster JG, Mahvi DM. A review of coaxial-based interstitial antennas for hepatic microwave ablation. *Crit Rev Biomed Eng* 2006;34(3):187–213.
11. Deardorff DL, Diederich CJ, Nau WH. Control of interstitial thermal coagulation: comparative evaluation of microwave and ultrasound applicators. *Med Phys* 2001;28(1):104–117.
12. Wolf FJ, Grand DJ, Machan JT, Dipetrillo TA, Mayo-Smith WW, Dupuy DE. Microwave ablation of lung malignancies: effectiveness, CT findings, and safety in 50 patients. *Radiology* 2008;247(3):871–879.
13. Oshima F, Yamakado K, Nakatsuka A, Takaki H, Makita M, Takeda K. Simultaneous microwave ablation using multiple antennas in explanted bovine livers: relationship between ablative zone and antenna. *Radiat Med* 2008;26(7):408–414.
14. Dong BW, Liang P, Yu XL, et al. Sonographically guided microwave coagulation

- treatment of liver cancer: an experimental and clinical study. *AJR Am J Roentgenol* 1998;171(2):449–454.
15. Liang P, Wang Y. Microwave ablation of hepatocellular carcinoma. *Oncology* 2007; 72(Suppl 1):124–131.
 16. Sun Y, Wang Y, Ni X, et al. Comparison of ablation zone between 915- and 2,450-MHz cooled-shaft microwave antenna: results in in vivo porcine livers. *AJR Am J Roentgenol* 2009;192(2):511–514.
 17. Knavel EM, Hinshaw JL, Lubner MG, et al. High-powered gas-cooled microwave ablation: shaft cooling creates an effective stick function without altering the ablation zone. *AJR Am J Roentgenol* 2012;198(3):W260–W265.
 18. Cavagnaro M, Amabile C, Bernardi P, Pisa S, Tosoratti N. A minimally invasive antenna for microwave ablation therapies: design, performances, and experimental assessment. *IEEE Trans Biomed Eng* 2011;58(4):949–959.
 19. Hines-Peralta AU, Pirani N, Clegg P, et al. Microwave ablation: results with a 2.45-GHz applicator in ex vivo bovine and in vivo porcine liver. *Radiology* 2006;239(1):94–102.
 20. Brace CL. Dual-slot antennas for microwave tissue heating: parametric design analysis and experimental validation. *Med Phys* 2011;38(7):4232–4240.
 21. Committee for the Update of the Guide for the Care and Use of Laboratory Animals; National Research Council. *Guide for the care and use of laboratory animals*. 8th ed. Washington, DC: National Academies Press, 2010.
 22. Cha CH, Lee FT Jr, Gurney JM, et al. CT versus sonography for monitoring radiofrequency ablation in a porcine liver. *AJR Am J Roentgenol* 2000;175(3):705–711.
 23. Schramm W, Yang D, Haemmerich D. Contribution of direct heating, thermal conduction and perfusion during radiofrequency and microwave ablation. *Conf Proc IEEE Eng Med Biol Soc* 2006;1:5013–5016.
 24. Ji Z, Brace CL. Expanded modeling of temperature-dependent dielectric properties for microwave thermal ablation. *Phys Med Biol* 2011;56(16):5249–5264.
 25. Coad JE, Kosari K, Humar A, Sielaff TD. Radiofrequency ablation causes ‘thermal fixation’ of hepatocellular carcinoma: a post-liver transplant histopathologic study. *Clin Transplant* 2003;17(4):377–384.
 26. Zhou Q, Jin X, Jiao D-C, et al. Microwave ablation: results in ex vivo and in vivo porcine livers with 2450-MHz cooled-shaft antenna. *Chin Med J (Engl)* 2011;124(20):3386–3393.
 27. Brace CL, Diaz TA, Hinshaw JL, Lee FT Jr. Tissue contraction caused by radiofrequency and microwave ablation: a laboratory study in liver and lung. *J Vasc Interv Radiol* 2010;21(8):1280–1286.
 28. Yu NC, Raman SS, Kim YJ, Lassman C, Chang X, Lu DSK. Microwave liver ablation: influence of hepatic vein size on heat-sink effect in a porcine model. *J Vasc Interv Radiol* 2008;19(7):1087–1092.